JOURNAL OF GEOPHYSICAL RESEARCH, VOL. 106, NO. B11, PAGES 26,365–26,378, NOVEMBER 10, 2001

# Random sequences of lithologies exposed on the Mid-Atlantic Ridge

Neil C. Mitchell[1]

Department of Earth Sciences, University of Oxford, Oxford, England, UK

**Abstract.** Magmatic, tectonic, and sedimentary processes at slow spreading ridges are known to create complex distributions of rock types at the surface that do not reflect the classical model for oceanic crust with horizontally stratified lithologic layers comprising extrusives, sheeted dikes, and gabbro overlying mantle rocks. A database of seafloor lithology observed in >100 submersible dives is analyzed in order to characterize this complexity. As a way of summarizing the relations between units exposed on rock slopes, the transitions between different lithologies are counted to create transition probability tables, which represent the relative likelihood of passing between different rock types. They reveal that extrusives exposed on Atlantic rock slopes crop out above dikes, serpentinite, and gabbro, in order of decreasing, though with similar, likelihood. Tables derived from the occurrences of the different rock types in dredge hauls are similar to the tables derived from dive observations, so the dredges record a similar heterogeneity. It is suggested that slope failure of gabbroic and ultramafic escarpments, implied by sedimentary breccias in off-axis drill sites, may contribute to the heterogeneity, in addition to the magmatic and tectonic processes that have been discussed extensively by previous workers. Further analysis of the tables reveals that the net effect of tectonic, magmatic, and sedimentary processes is to produce a distribution of rock types that is indistinguishable from a random distribution. This result is derived from the immediate transitions between units and therefore applies to the fine-scale structure. If oceanic crust is also heterogeneous on a larger scale, however, it could have more general implications for resolving different crustal models. For example, the presence of a sheeted dike layer is critical evidence for continuous seafloor spreading, but its presence or absence in any one location may be an artifact of the heterogeneity or discontinuous exposure. Methods will therefore be needed to characterize large-scale heterogeneity so that the significance of these large-scale observations can be assessed.

## 1. Introduction

The view developed in the 1970s by comparing some ophiolite sequences with the apparently layered structure in seismic refraction experiments was that the oceanic crust is horizontally stratified with basaltic lava overlying sheeted dikes, gabbro, and ultramafic rocks, respectively (Figure 1a) [*Penrose Conference Participants*, 1972]. Studies on the Mid-Atlantic Ridge have since shown that slow spreading oceanic crust probably has a more complex structure because all four rock types are found at the surface in many different configurations [e.g., *Karson*, 1998]. At least two explanations for exposures of lower crustal and mantle rock types can be put forward. First, where oceanic crust is thin near transform faults, normal faulting is able to bring deep lithologies (gabbro and peridotite) to the surface, but otherwise faulting disrupts an originally stratified crust [*Dick et al.*, 1991; *Fox et al.*, 1980; *Francheteau et al.*, 1976; *Karson*, 1990; *Tucholke and Lin*, 1994]. Second, the crust near segment ends or in areas with low magma supply consists of a heterogeneous assemblage of gabbroic intrusions and serpentinized peridotite overlain by a thin carapace of basaltic lava, and faulting easily exposes deep rock types (Figure 1b) [*Cannat*, 1996; *Cannat et al.*, 1995; *Dick*, 1989; *Lagabrielle et al.*, 1998; *Lagabrielle and Cannat*, 1990]. More recently, data from sonars combined with sampling have revealed that large-offset faults are capable of elevating deep rock types, such as peridotite and gabbro, to the seafloor [*Blackman et al.*, 1998; *Cann et al.*, 1997; *Tucholke et al.*, 1998]. A distribution of lithologies similar to that shown in Figure 1b could therefore arise locally by eruption of lava over a low-angle fault surface and uplift of a klippen of the fault hanging wall [*Karson and Laurence*, 1997a]. The two models in Figure 1 represent end-members: in the first, continuous spreading leaves a continuous sheeted dike layer, whereas in the second (because of faulting or complex magmatic history) the sheeted dike layer is absent.

Steep fault escarpments found in transform valleys and rifts have been proposed to provide deep sections, termed "tectonic windows" [*Fox et al.*, 1980], that are useful for viewing the internal structure of oceanic crust. Intensive dredging and submersible diving campaigns have been carried out in these areas attempting to address crustal structure [*Auzende et al.*, 1989; *Karson and Dick*, 1983; *Mevel et al.*, 1991]. The spatial distribution of rock units and their geological histories revealed by fabrics and mineralogy are important for deciphering the origins of crustal components. The nature of the contacts between units, whether igneous, tectonic, or sedimentary, is also important, but contacts are commonly obscured by sediments and talus, by thick manganese coatings on older crust, and by later faulting. The quality of the observations of contacts also depends

[1]Now at Department of Earth Sciences, Cardiff University, Cardiff, Wales, UK.

Copyright 2001 by the American Geophysical Union.

Paper number 2001JB000241.
0148-0227/01/2001JB000241$09.00

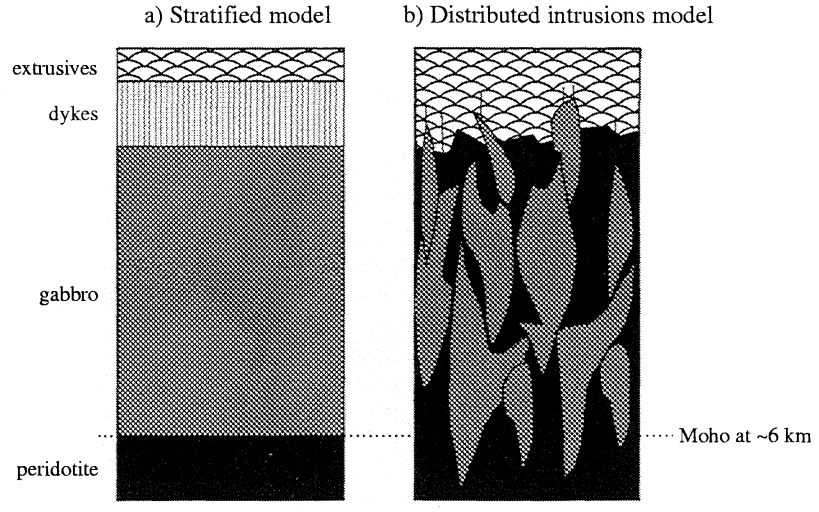


**Figure 1.** (a) The classical model of oceanic crust with stratified layers of extrusives, dikes, gabbro, and ultramafic rocks [*Penrose Conference Participants*, 1972]. (b) A model in which the middle and lower crust consists of small gabbroic intrusions with screens of variably serpentinized peridotite [*Cannat*, 1993]. A carapace of extrusives, breccias, and minor dikes overlies the plutonic layer.

on the abilities of dive scientists and time available to maneuver the submersible around contacts, so observations are unlikely to be consistent.

In view of the above difficulties, a different approach is attempted here. The nature of contacts between units is ignored, and instead the transitions between different rock types observed in all the available Atlantic dives are used to generate transition probability tables, using methods originally developed to study sedimentary sequences [*Potter and Blakely*, 1968; *Selley*, 1969]. The dive data provide an imperfect database for such a study compared to sedimentary sequences, given the variable talus and sediment cover, observational inconsistencies, and difficulty in developing a discrete lithological classification based on partly subjective dive observations. Nevertheless, if faults expose a characteristic sequence of rock types, the transition probability tables should record such a sequence if it is particularly common. In other words, the tables provide a test of whether there is a common sequence or not, and they provide a way of assessing competing crustal models. Both dive data and rock dredges are biased by researcher's interests in sampling scarps where rock sequences are best exposed, avoiding flat sedimented areas, and preference for lower crustal and mantle exposures. Information from dredges are compared to the dive data because the dredges form a much larger database and are found to support the conclusions based on the dives. Deep drilling through ultramafic and gabbroic sequences in off-axis settings also provides clues to the origins of exposures of deep lithologies [*Juteau et al.*, 1990], which are discussed along with the transition tables.

A general problem with complex geological observations is how to assess their significance, particularly for slow spreading oceanic crust where heterogeneity leads to different lithologic structures being found in different places [*Karson*, 1998]. The study presented here was motivated to summarize the geological observations using graphical methods based on tables, which could also be tested using statistics. It is recognized, however, that in reducing the diversity of available information from the dives to simple lithological classes, a great deal of the original dive information is lost and statistical tests only provide ways of assessing the numerical correspondence of data, not the correspondence that may exist in metamorphic or tectonic history, geological context (origin of an explosure by faulting, for example), etc. Nevertheless, despite these limitations, it is hoped that this study will provoke some thought into how the significance of geological observations from dive campaigns can be reliably assessed and, given the heterogeneity observed, how best to proceed with further observations.

## 2. Origins of Lithologic Heterogeneity in Slow Spread Crust

Various magmatic, tectonic and sedimentary processes contribute to the chaotic distribution of rock types observed at the surface. The uplift of serpentinized peridotites and gabbros to shallow crustal levels probably occurs in the footwalls of large-offset normal faults ("detachment faults"), usually, though not exclusively, at segment ends. This tectonic origin was inferred south of the Kane transform valley at Ocean Drilling Program (ODP) Sites 920-924 [*Dick et al.*, 1981; *Karson and Lawrence*, 1997a; *Karson and Lawrence*, 1997b; *Mevel et al.*, 1991] and is suggested by 16-35 km wide fault surfaces in sonar images [*Blackman et al.*, 1998; *Cann et al.*, 1997; *Mitchell et al.*, 1998; *Tucholke et al.*, 1996]. Uplift by discrete faults, rather than diapirism, is also implied by fabrics in core and dredge samples [*Cannat*, 1993; *Jaraslow et al.*, 1996] and because these serpentinites have similar density to gabbro [*Karson and Lawrence*, 1997a]. If the crust beneath some parts of the median valley floor consists of ultramafic screens intruded by gabbroic plutons (Figure 1b) [*Cannat*, 1993; *Sleep and Barth*, 1997], the ultramafic component probably arrives there by tectonic uplift followed by spreading of the fault footwall by intrusions or by a change in the sense of faulting leaving footwall ultramafics in the hanging wall of the new fault, as implied by serpentinite exposed on both flanks of the ridge axis near 15°20'N [*Cannat et al.*, 1997]. Thus ultramafic exposures can result from a complex sequence of tectonic and magmatic events. Gabbroic intrusions may be small and ephemeral [*Barclay et al.*, 1998; *Bloomer et al.*, 1991; *Kong et al.*, 1992; *Nisbet and Fowler*, 1978; *Pederson*, 1986], so intrusions likely create complex relationships among

gabbro, ultramafic rocks, and any overlying dike complexes, leading to numerous contacts between gabbro, serpentinite, and dikes in exposures on scarps. Serpentinites and gabbro commonly outcrop immediately below extrusives on slopes [*Auzende et al.*, 1989; *Karson*, 1998; *Lagabrielle et al.*, 1998], creating transitions between gabbro, serpentinite, and extrusives. Although contacts are commonly obscured, it seems likely that some of these extrusive units are klippen of hanging wall rocks uplifted by the fault [*Tucholke et al.*, 1998], as also implied by the basalts at Deep Sea Drilling Project (DSDP) Sites 556 and 558 described in section 6.

## 3. Dive Observations Database

The database (Figures 2 and 3) [*Mitchell et al.*, 2000] consists of seafloor topography along dive profiles measured from published reports given in the electronic supplement[1] to this paper. The geology along each profile was classified into extrusives, dikes, gabbro, and serpentinite (E, D, G, and S, respectively) on the basis of the interpretational cross sections, geology, and sample descriptions in the reports. "Serpentinite" includes all ultramafic lithologies including any possible ultramafic cumulates. "Dikes" includes massive diabase outcrops and dike swarms as well as sheeted dike complexes. In the analysis, talus of a particular lithology and in situ outcrop of that lithology were not discriminated because shallow talus cover over in situ rock and variable sediment cover can make them difficult to tell apart consistently by different observers working from the limited view within a submersible. If talus covers extensive areas, this could potentially lead to anomalous lithologies in the database derived from upslope, although the original observations used to produce Figure 3 suggests that this is not a problem (possible effects of landslides on dredge data are discussed in section 7.2).

The spatial extents of igneous rock types can vary over many different scales, down to individual intrusive veins only centimeters wide, so a consistent resolution limit to the classification should ideally be defined. The data resolution, however, reflects the observers' difficulties in mapping geology with varying sediment, talus cover, and manganese coating and also varies with the scale and quality of the published dive figures. In this classification, small outcrops, such as individual dikes or isolated talus of erratic lithology, were deliberately ignored so that the resolution is coarser than 100 m. Figure 4 (bottom four graphs) shows histograms of the horizontal extents of each lithology in the Atlantic dive data (Figure 3), which contain no ultramafic, gabbro or sheeted dike units narrower than 100 m and only a few dike and gabbro units narrower than 200 m. Figure 4 (top) shows the cumulative distribution of all the Atlantic units expanded to show the initial 1 km and reveals that only 1.5% of the units (basalts) are narrower than 100 m. Some small units were omitted in the digitizing process but were effectively reentered by including supplementary transitions when generating the transition probability tables (section 4). The adjusted data (profiles 26, 31, 33, 38, 39, 62, 64, 91, and other supplementary data described in section 4) had no units narrower than 100 m. Dive locations were classified by tectonic environment into areas near transform faults (on transform valley walls or anywhere within 20 km of transform faults including inside-corner massifs) and areas away from transform faults but including dives near nontransform discontinuities. Although a few published profiles were omitted in compiling Figure 3, they were profiles covering basalt only with no transitions to other lithologies, and their extents were taken into account when computing the abundances of section 4.

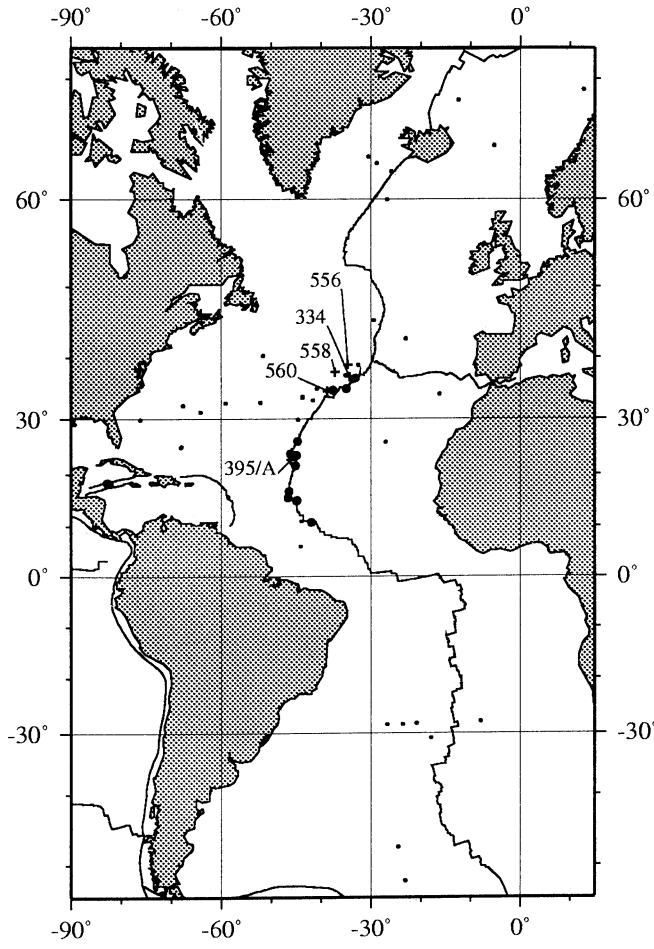


**Figure 2.** Locations of submersible dives (large dots) studied here with plate boundary from *Muller et al.* [1997]. Crosses and associated numbers mark DSDP and ODP sites where off-axis drilling recovered gabbro and ultramafic rocks, and small dots mark sites where only basalt was recovered.

## 4. Comparison of Lithological Abundances in the Dive Data With Dredge Hauls

Comparing the different data types is useful for assessing their relative sampling bias. Figure 5 shows lithologic abundances calculated from the dredge haul reports mentioned in the caption. Sets 14-16 show abundances calculated from the horizontal extents of each lithology observed in the dives (Figure 3). Dives are often spatially clustered, so distances were inversely weighted by the number of dives in each 20 km by 20 km area (a size chosen as it roughly encompasses typical massifs of intrusive rocks [*Gracia et al.*, 1997]). It should be noted, however, that weighting will help to reduce the effect of sampling bias but will

[1]Supporting material is available via Web browser or via Anonymous FTP from ftp://agu.org, directory "apend" (Username="anonymous", Password="guest"); subdirectories in the ftp site are arranged by paper number. Information on searching and submitting electronic supplements is found at http://www.agu.org/pubs/esupp_about.html.

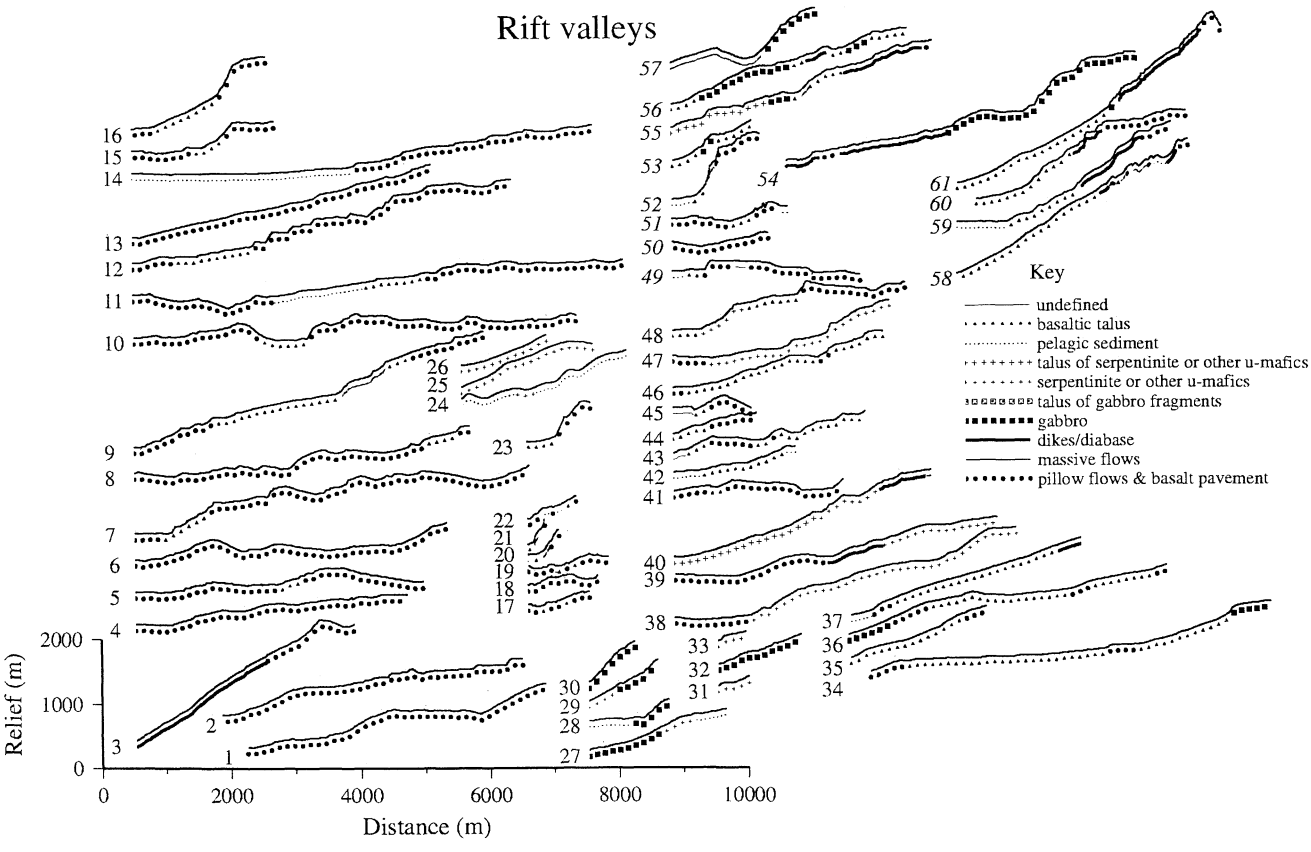


**Figure 3a**. Rift valley walls or crestal mountains, including massifs near nontransform discontinuities of the ridge axis. Submersible observations from the sources given in the electronic supplement to this paper and located in Figure 2 are shown with no vertical exaggeration. Profiles from medium or fast spreading ridges (not used in this study) are shown with italicized numbering.

not completely remove it; bias can only be fully avoided by systematic sampling. Some data not originally incorporated in Figure 3 or published in map form only [*Cannat et al.*, 1997; *Stroup and Fox*, 1981] were used to measure horizontal extents of lithologies, and these data were also incorporated into sets 14-16. The total dive distances are 142, 202, and 344 km for sets 14, 15, and 16. Note that sets 10-13 show relative abundance in dredge hauls by mass, whereas sets 1-9 give relative abundance by separately counting the number of dredge hauls recovering basalt, diabase, gabbro, and ultramafics in turn and then normalizing the sum of all counts to 100%. Differences between abundances calculated by the two methods reflect the size of particular lithologic samples in hauls and possibly therefore the size of rock bodies on the seafloor or their susceptibility to dredging. The abundances calculated by the number of dredge hauls that they occur in clearly can only be qualitatively compared to dive abundances calculated by distance. The dive abundances are more readily compared to the dredge abundances by mass.

The dive data should be compared with dredge results from the appropriate tectonic setting. Set 14 should be compared with sets 1, 2, 4, 9, 10, 11, and 13, which are from transform valley walls or adjacent transform-parallel ridges. Sets 3 and 12 are from the rift valley walls and crestal rift mountains, which can roughly be compared with set 15. The combined dive data set (set 16) may be compared with set 8, which represents a relatively systematic off-axis sample mostly from dredging. Set 5 represents samples largely from within 30 km of transform valleys, including samples from the axial rift valley. While it may suffer from underreported basalt [*Tucholke and Lin*, 1994], this is the largest sample set and can be compared with set 14.

There may be differences of interpretation between the dredge and dive data which arise because submersible observers are able to interpret surface morphology (e.g., lava flow textures, sheeted dikes), whereas dredged rocks can sometimes only be interpreted based on petrology and geochemistry. (Figure 5 shows lithologies using petrological termininology, whereas the later transition probability tables show them using terminology based on the dive observations.) Comparison between the two data types is inexact because of the possibility of basaltic dikes or diabase in massive flows.

The dive abundances by distance were tested against the dredge abundances by mass (sets 13 and 14), assuming that each 1 km distance of dive observation represented an independent sample of lithology. Sets 13 and 14 were considered the most equivalent to each other given their tectonic settings, and the dredge sampling strategy and assuming that dredge abundances by mass are equivalent to dive observations by distance. The extrusive and dike classes in the dive data and the basalt and diabase classes in the dredges were combined to account for potential interpretation differences. The following goodness-of-fit statistic [*Miller and Freund*, 1965, p. 202] was calculated, where $A_1$ to $A_3$ are the dive distances containing extrusives plus dikes, gabbro, and serpentinite, respectively, and $B_1$ to $B_3$ are the corresponding masses of those lithologies in the dredge hauls:

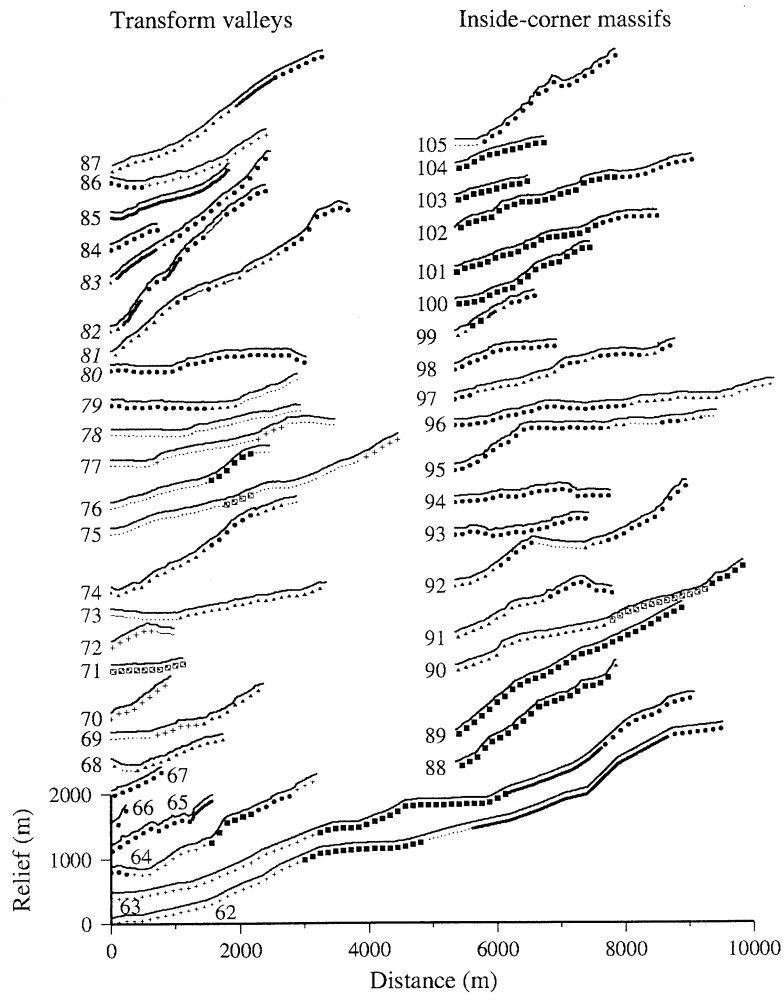


**Figure 3b.** Sections from transform valley walls. Profiles 88-105 are from slopes within 20 km of transform valleys, mostly on the massifs adjacent to ridge-transform intersections. Submersible observations from the sources given in the electronic supplement to this paper and located in Figure 2 are shown with no vertical exaggeration. Profiles from medium or fast spreading ridges (not used in this study) are shown with italicized numbering.

$$\chi_1^2 = \sum_{i=1}^{3} \frac{(A_i - e_i)^2}{e_i}, \qquad (1)$$

where $e_i = B_i \Sigma_i A_i / \Sigma_i B_i$. $A_1$, $A_2$, and $A_3$ were scaled so that their sum equaled the total dive distance (142 km). Equation (1) yielded $\chi_1^2 = 33.6$, greater than $\chi_1^2 = 5.99$ expected for the 5% level (2 degrees of freedom) and suggesting that they are statistically different. However, it is perhaps more significant that the two data sets are qualitatively similar apart from their basalt abundances, which may reflect basalt rubble often found on rock slopes of other lithologies but ignored in the dive classification. Although it has been suggested that gabbro and serpentinite have different susceptibility to dredging [*Dick et al.*, 1991], these two rock types show similar ratios for sets 13 and 14 in Figure 5. Diabase may be underrepresented in the dive data because small veins and dikes were ignored in the classification. Because the submersible dives most likely underrepresent the areas of flat-lying basaltic seafloor relative to fault scarps, set 16 for all Atlantic seafloor provides upper bounds on the surficial extents of gabbro and serpentinite (8% and 22%, respectively).

Most off-axis drilling sites were originally chosen without prior knowledge of the lithologies likely to be found there, so they form a relatively unbiased sample. The overwhelming majority have recovered basalt only. A survey of all the site reports for the DSDP and the ODP, ignoring sites obviously on aseismic volcanic ridges, found that 46 Atlantic sites recovered basalt only (small circles in Figure 2). Considering that only three sites had ultramafic or gabbroic rocks at the basement surface (Sites 395, 395A, and 560; section 6), the occurrence of plutonic rocks is only 6%, which is much less than in the dredge and dive data (Figure 5). None of the Atlantic off-axis site reports mention massive gabbro at the basement surface. The sites where plutonic rocks were recovered are relatively near-axis (Figure 2) and were deliberately drilled into basement (most sites were intended to drill the sedimentary section only), so possibly some of the basalt-only sites may have sampled a thin veneer of basalt over plutonic rocks.

## 5. Transition Probability Tables

Lithologic transition probability tables were generated by counting transitions down slope in the dive profiles (Figure 3). The procedure ignores whether the profiles run down in situ rock slopes exposed by individual faults, talus, or terraces between faults because segmenting the profiles would require high-

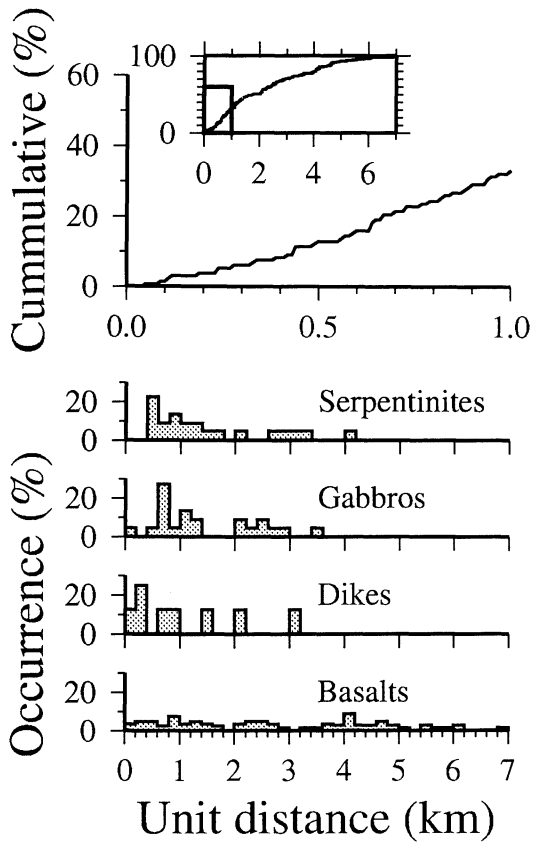


**Figure 4.** Horizontal extents of lithologic units for the Atlantic dives in Figure 3 to illustrate data resolution. (bottom four graphs) Histograms of the extents of the four classified types, including talus of those lithologies, binned in 200 m intervals. (top) The first 1 km of the cumulative distribution for all the lithologic units; only 1.5% of the units (all basalt) are <100 m. Inset shows the part of the full histogram that is plotted. Note that these graphs show only the extents within each dive profile, not the true lateral extents of units which commonly extend beyond individual profiles.

resolution sonar data, which are not available for most of the sites. Segmenting profiles would also be difficult because scarps are often composed of many individual fault line scarps [*Karson*, 1998]. All the four lithologies occur at different depth levels in the profiles, as seen in dredge hauls in transform valleys [*Francheteau et al.*, 1976], so the transitions were counted starting from each of the four lithologies. (Note from the profiles in Figure 3 that all four lithologies can crop out at the tops of slopes so it is not strictly correct that lava always overlies the other lithologies. It might be possible to demonstrate that lava overlies them stratigraphically if the mapping were continued beyond the scarp crests so that their contacts with lava or other lithologies could be properly characterized, but dive time constraints usually prevent this.)

The lithologies encountered following each reference lithology are shown as simple proportions in each row of Figures 6a and 6b. The starting lithology (transiting from) is shown along the left of the convention (bottom left in Figure 6). Using Figure 6a (top) as an example, the bottom row for transitions starting from extrusives shows a sequence white, light shading, dark shading, medium shading representing 0% E->E, 17% E->D, 59% E->G, and 24% E->S (the E->E transition frequency is 0% because transitions from a lithology to itself are not allowed in this analysis). In other words, where extrusives crop out topographically above another lithology, that second lithology is most commonly gabbro, second commonly serpentinite, and least commonly dikes.

Sedimented sections of dives were ignored where they lie between different rock types so that only single transitions were recorded. Some data had not been included in Figure 3 or were originally published in map form only [*Auzende et al.*, 1994; *Cannat et al.*, 1997; *Stroup and Fox*, 1981]; to improve sample size, down slope transitions were interpreted from them and included in the tables. The second (lower) rows of tables in Figures 6a and 6b show the tables calculated with the transitions weighted inversely by the number of dives in each 20 km by 20 km area. These weights and the transitions interpreted from the dive profiles are given in the electronic supplement to this paper.

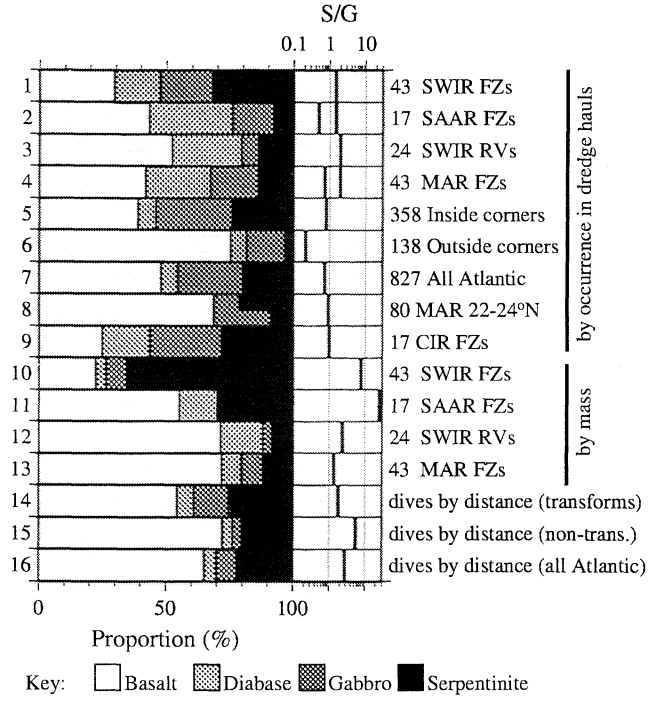


**Figure 5.** Relative abundances of lithologies in dredge hauls and dives. Numbers of hauls are given to the right of each set. Sets 1-4 and 10-13 are from *Dick* [1989], 5-7 are from *Tucholke and Lin* [1994], 8 is from *Cannat et al.* [1995] (basalt and diabase combined as one class and split gabbro and ultramafic segment representing where both these types were recovered), and 9 is from *Engel and Fisher* [1975]. Sets 14-16 show abundances calculated by horizontal dive distance and weighted inversely by number of dives per 20 km by 20 km area. Legend represents Southwest Indian Ridge fracture zones (SWIR FZs), Southwest Indian Ridge rift valley walls (SWIR RVs), South American Antarctic Ridge fracture zones (SAAR FZs), Mid-Atlantic Ridge fracture zones (MAR FZs), and Central Indian Ridge fracture zones (CIR FZs). The graph on the right shows the ratio of serpentinite (S) to gabbro (G) with a logarithmic scale. Of the data compiled by *Tucholke and Lin* [1994], only 9% were taken from papers on submersible dives, so sets 5-7 mostly represent dredge reports. The *Cannat et al.* [1995] survey included some dive and drill core samples. Basalt and diabase are combined as one class in the *Cannat et al.* [1995] sample survey. Note the general correspondence between sets 13 and 14, which both represent areas around transform valleys.

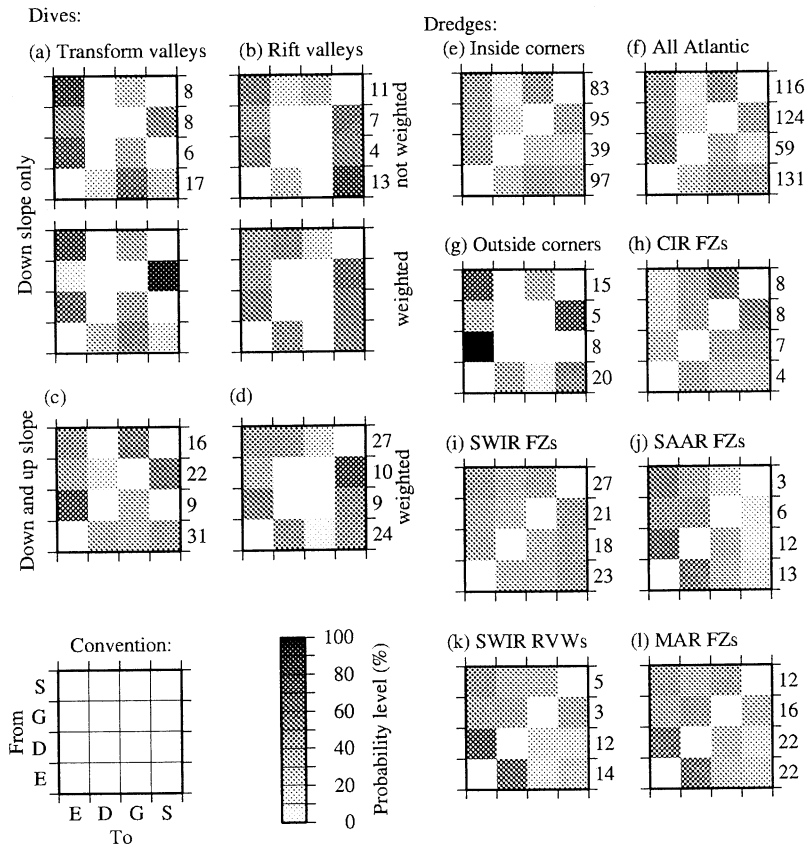


**Figure 6.** Probability tables representing transitions between lithologies in dives (convention given at bottom left) and cooccurrences of lithologies in dredge hauls. Shading in each row shows the relative frequency of transitions from the lithology given on the left to those listed below each table (from extrusives, E, dikes, D, gabbro, G, or serpentinite, S). In Figures 6a and 6b the transitions were counted down each dive profile (increasing water depth) with weightings given in the supplementary data to this paper. In Figures 6c and 6d the transitions were counted both up and down slope. Numbers to the right of Figures 6a-6d are the total number of transitions counted (those in Figures 6c and 6d are "doubled up" by counting both up and down slope). The dredge tables in Figures 6e-6l were derived by counting the number of times dredges brought up each lithology with a particular reference lithology (using basalt, diabase, mafic plutonic rocks, and ultramafic rocks as E, D, G, and S). Numbers to the right of Figures 6e-6l are the number of dredges contributing to each row. The data for Figures 6e-6g are from Table 1 of *Tucholke and Lin* [1994], with the "All Atlantic" table (Figure 6f) derived from the areas they classed as "inside corners," "outside corners," and "undetermined." The data for Figure 6h are from *Engel and Fisher* [1975], and data for Figures 6i-6l are from *Dick* [1989]. Legend represents Southwest Indian Ridge fracture zones (SWIR FZs), South America Antarctica Ridge fracture zones (SAAR FZs), Southwest Indian Ridge rift valley walls (SWIR RVWs), and Mid-Atlantic Ridge fracture zones (MAR FZs).

The tables in Figures 6a and 6b (weighted) were combined to form a single table which is summarized in Figure 7 as a tree diagram in which the numbers represent the transition frequencies in percents. Thus the combined data set shows that extrusives outcrop above dikes, gabbro, and serpentinite with similar frequency. In Figure 6a (weighted table), E→G is more common than E→S, in contrast to the table in Figure 6b. However, this probably reflects the small sample size since the tendency is lost when the tables in Figures 6a and 6b are combined to form that illustrated in Figure 7.

To compare with dredge hauls, Figures 6c and 6d show tables generated including counts both up and down slope. Figures 6e-6l show co-occurrence tables constructed for dredge hauls by counting the number of hauls in which each lithology occurs with a particular reference lithology. The two types of data are not exactly equivalent because of the problem of terminology mentioned in section 4 and because multiple lithologies in dredges imply that they are only in general association (depending on the dredged distance, which is rarely reported), not necessarily that they are juxtaposed. The dredge haul tables are, however, useful for illustrating lithological associations and generally support the inferences based on the dives.

The dive table in Figure 6c was tested against the dredge tables to see if they represent similar populations using the following statistic [*Miller and Freund*, 1965]:

$$\chi_2^2 = \sum_{i=1}^{4}\sum_{j=1}^{4} \frac{\left(C_{ij} - e_{ij}\right)^2}{2e_{ij}}, i \neq j, \qquad (2)$$

where $C_{ij}$ are the number of dredge hauls containing lithologies $i$ and $j$ and $D_{ij}$ are the number of dive observations of contacts between lithologies $i$ and $j$ ($i,j$=1 to 4 represent basalt/extrusives, diabase/dikes, gabbro, and ultramafic rocks, respectively). The

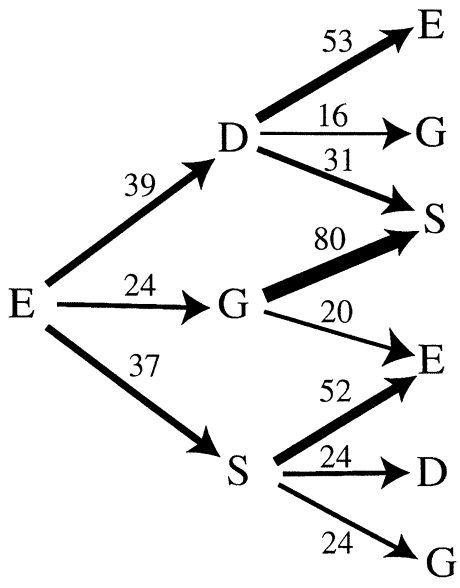


**Figure 7.** Tree diagram illustrating the weighted transition probability tables in Figures 6a and 6b combined (Figure 12c (left)). The numbers represent the percentage frequencies of each transition counted downslope and widths of arrow shafts are proportional to transition frequencies. The figure shows that extrusives crop out above dikes, gabbro and serpentinite with similar frequencies.

dredge haul counts expected based on the dive table are $e_{ij}=D_{ij}\Sigma_{ij}C_{ij}/\Sigma_{ij}D_{ij}$, excluding the diagonal elements ($D_{i=j}=0$). The factor of 2 was included because the dredge tables are symmetrical ($C_{ij}=C_{ji}$). The differences were deemed to be significant if the calculated $\chi_2^2$ value was >11.07 (5% level for 5 degrees of freedom).

Testing the table in Figure 6c (weighted) against the tables in Figures 6e and 6l yielded $\chi_2^2$=45.1 and 20.7, respectively, suggesting that they are statistically different. However, given that dredge hauls provide imperfect recording of transitions and the small number of counts in the dive table (containing <5 counts in some elements), it is more important that both kinds of data show common associations, for example, between extrusives and serpentinite. Figure 8 compares a table derived by combining the data from all the Atlantic dives (Figures 6c and 6d) with the table in Figure 6f (reproduced in Figure 8b), which has the largest sample size. Although they are statistically different ($\chi_2^2$=115), both data sets show associations between all four lithologies.

## 6. Stratigraphy at Atlantic Off-Axis Drill Sites

The deep lithologies recovered at these sites were mostly gabbroic and serpentinite sedimentary breccias, suggesting that slope failures cause significant redistribution of these lithologies. On the basis of the DSDP site reports, this section reviews the six Atlantic off-axis sites where deep lithologies were recovered [*Juteau et al.*, 1990] and reassesses their origin on the basis of their tectonic context revealed by the marine gravity field [*Sandwell and Smith*, 1997]. Figure 9 summarizes their stratigraphy. For Site 334, the lithologies shown below the extrusives are the sections cored only, whereas the other sites are illustrated more schematically without gaps between cored samples. The effects of slope failures on apparent crustal heterogeneity are discussed in section 7.2.

Sites 334 and 560 were drilled at the base of steep fault scarps [*Aumento and Melson*, 1977; *Bougault and Cande*, 1985; *Cande et al.*, 1985] away from transform valleys. The stratigraphy of the Site 334 plutonic rocks shown in Figure 9 reveals a chaotic distribution of rock types that most likely represents debris avalanche or other deposits caused by failure of a scarp of plutonic rocks, which were subsequently overlain by valley floor lavas [*Juteau et al.*, 1990]. Site 560 penetrated a serpentinite and gabbro breccia, which was probably also created by slope failures. Breccias at both sites contain calcareous sediments.

Sites 556 and 558 are possible candidates for drilling over detachment fault surfaces [*Blackman et al.*, 1998; *Cann et al.*, 1997; *Dick et al.*, 1981; *Karson*, 1990; *Mevel et al.*, 1991; *Mitchell et al.*, 1998; *Tucholke et al.*, 1998]. Site 556 penetrated a surface dipping gently by 150 m in 15 km to the west, which ends westward in an axis parallel valley [*Sandwell and Smith*, 1997]. The Site 556 report describes a gabbroic breccia with serpentinized matrix overlain by basalts [*Bougault and Cande*, 1985]. The breccia is probably sedimentary, although no calcareous sediment was found in the matrix. Site 558 penetrated a gently east dipping basement [*Bougault and Cande*, 1985, p. 129] adjacent to a series of basins of a nontransform discontinuity [*Sandwell and Smith*, 1997]. The Site 558 report describes the serpentinized gabbro and serpentinite section (shown as breccia in Figure 9) as highly sheared and having a mylonitic fabric, consistent with a fault origin. Their underlying serpentinites are described as strongly sheared and mylonitic. The stratigraphy at these two sites could be explained by detachment faults bringing lower crustal and mantle rocks to the seafloor, while the overlying ~100 m of basalts at the two sites represent either later eruptions or klippen of axial valley lavas carried by the faults, as suggested for basalts outcropping above serpentinite near ODP Site 920 [*Karson and Lawrence*, 1997a]. The Site 556 gabbroic breccia would then probably represent material mobilized on the detachment fault slope when exposed

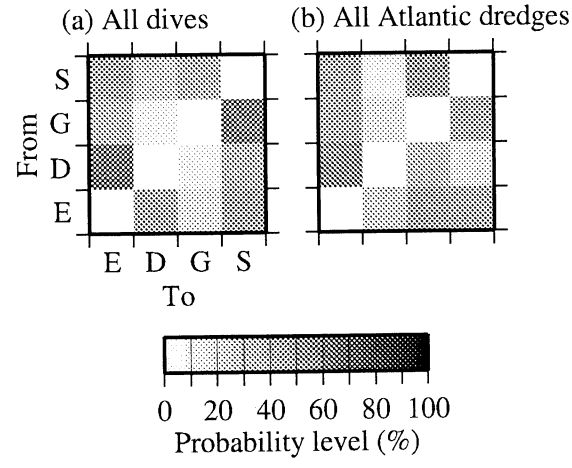


**Figure 8.** A comparison of tables derived from the Atlantic dive observations with dredge hauls. (a) Combined transitions for all Atlantic dives, including counts both up and down slope, and with counts weighted inversely by the number of dives in each 20 by 20 km area (i.e., combined table of Figures 6c and 6d). (b) A table of joint occurrences of lithologies in all the Atlantic dredge data from Figure 6f [*Tucholke and Lin*, 1994]. Note the general similarity suggesting similar associations between the four rock types.

on the seafloor, as seen on gabbroic and serpentinite fault slopes at the modern axial valley [*Karson and Lawrence*, 1997a, 1997b], rather than a tectonic breccia.

Breccias at Sites 395 and 395A probably also represent slope failure deposits [*Juteau et al.*, 1990; *Melson and Rabinowitz*, 1979] and consist of serpentinite, gabbro, and basalt clasts with some carbonate matrix, separated by basalt units. Most likely, the sequence represents intermittent mass wasting of a plutonic escarpment into the volcanically active median valley [*Juteau et al.*, 1990; *Melson and Rabinowitz*, 1979]. The sites lie within an east-west series of basins [*Hussong et al.*, 1979; *Sandwell and Smith*, 1997] of the off-axis trace of a nontransform discontinuity [*Schulz et al.*, 1988] but are anomalous in that they occur on an outward (west) dipping basement slope.

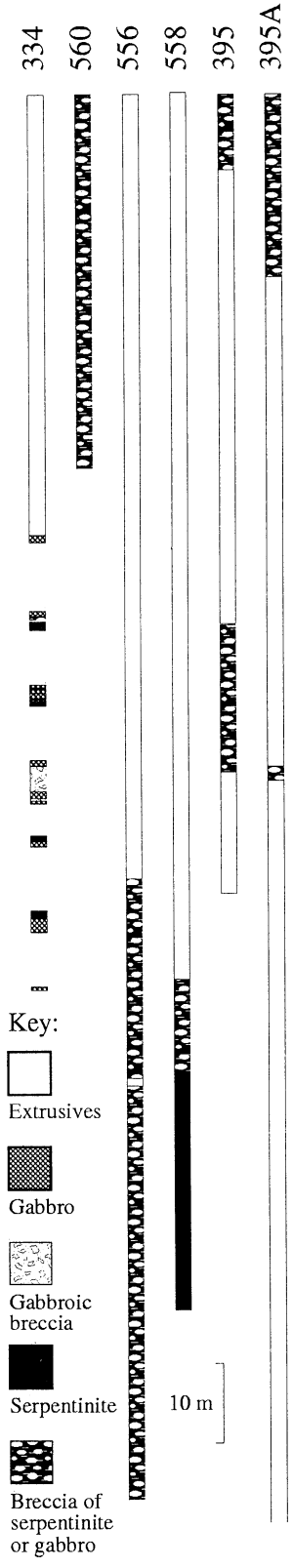


## 7. Discussion

### 7.1. Transition Probability Tables and Crustal Models

The transition tables can be assessed against exposures likely to be created by steep normal faulting of the two crustal models introduced earlier. This assessment is not ideal because a given table could be produced by many different configurations of rock types, that is the tables provide nonunique characterizations of structure. Nevertheless, it does illustrate how tectonic and magmatic processes may lead to the characterized heterogeneity.

In Figure 10a, normal faults expose contacts between extrusives and dikes, which would then dominate the transition probability tables. Other contacts with gabbro and serpentinized peridotite are possible if faults are large enough or if the crust is thin as in fracture zones [*Fox et al.*, 1980]. The 39% probability of E→D compared to E→S and E→G (Figure 7) partly supports this model. However, even allowing for mixing of units by scarp slope failures, the full diversity of lithologic associations in the Atlantic dive and dredge tables (Figure 6) are unlikely to have been produced by this kind of model. Only one Atlantic dive transect recording the complete classical stratigraphy in Figure 10a has been reported (Vema fracture zone [*Auzende et al.*, 1989]).

In Figure 10b a crust of plutonic rocks is overlain by a carapace of extrusives and minor dikes. Faulting of this model crust results in abundant contacts between extrusives, gabbro, and serpentinite. The model transition table has high probability in the E→G and E→S elements and in the opposite corner, much like the observed dive and dredge tables (Figure 6). The transition probability tables therefore reflect the common outcropping of extrusives immediately above plutonic and ultramafic units [*Karson*, 1998] and are at least not inconsistent with the model in Figure 10b. Failure of these slopes (dashed lines in Figure 10b and illustration to the right) would likely further emphasize these associations (the effect of slope failure on the tables in detail depends on whether the slope fails instantaneously or by progressive erosion [*Mitchell et al.*, 2000]). The high E→D probability in Figure 7 arises from dike swarms in a small number of dives, which are relatively isolated and

**Figure 9.** Lithologic summary of the six Atlantic off-axis DSDP sites that recovered ultramafic and gabbroic rock types. Sites 334 and 560 were drilled onto east dipping slopes, and breccias probably represent deposits from slope failure of fault scarps. For Site 334, only the cored intervals are shown without interpolation (gaps represent unsampled intervals). The chaotic distribution of rock types at Site 334 probably represent blocks of a debris avalanche deposit (breccia units for the other sites are shown more schematically). Sites 556 and 558 lie on more gently dipping slopes and are interpreted as possible drilling of detachment fault surfaces. Sites 395 and 395A probably also represent drilling of mass-wasting deposits interlayered with lava [*Juteau et al.*, 1990].

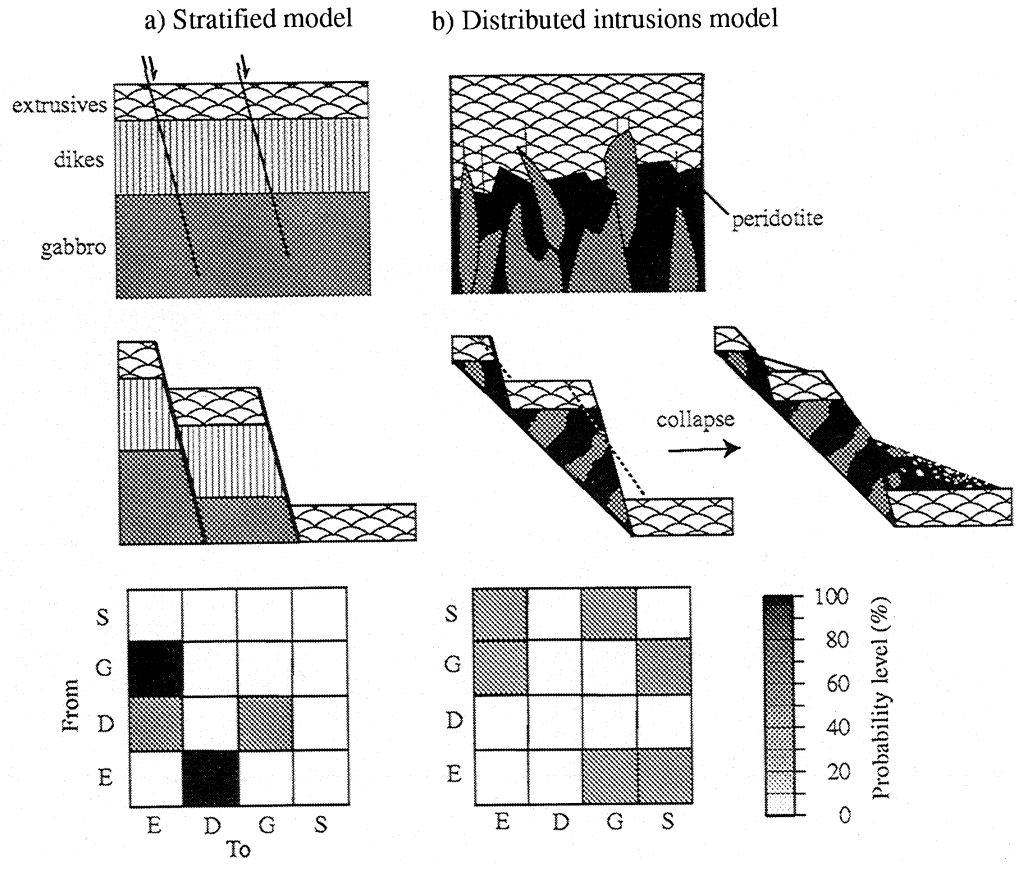


**Figure 10.** Transition probability tables expected from the alternative crustal models in Figure 1. (a) High-angle faulting of a stratified crust leading to contacts between E and D and perhaps also with G if fault heave exceeds the dike and extrusive layer thickness. (b) Extrusives emplaced directly over a deep intrusive complex with few feeder dikes exposed, leading to a slope section containing contacts between E, G, and S (contacts with D omitted for simplicity). Slope failure, erosion, and development of talus fans (represented by the dashed lines and illustration to the right) would probably further complicate the sequence.

consequently have high weighting (3, 37-40, 62, 63, 65). Without the weighting, the E→D transition probability is only 20%. Many of the Atlantic diving campaigns have concentrated on areas where gabbro and serpentinite are exposed, but determining the extent to which some of the dike swarms form coherent bodies will need more systematic mapping of them.

Figure 11 shows two models looking into the side of a transform valley wall intended to simulate some effects of large-offset low-angle ("detachment") faults [*Cann et al.*, 1997; *Tucholke et al.*, 1998]. In model A (5X vertical exaggeration) a detachment fault on the left has exposed a layered sequence of extrusives, dikes, gabbro, and serpentinite on an inside-corner massif and is overlain on the left by more recent extrusives. The fault, which is 20° within the crust, has rotated to the horizontal so that crustal layers are tilted 20° to the right. In being uplifted from the rift valley floor onto the inside-corner high, the structure is offset by a 500-m throw high-angle normal fault (perpendicular to the detachment fault surface and parallel to the transform and to the page), such as probably occur in transform valley walls [*Francheteau et al.*, 1976]. The model dredge lithologies (Figure 11b) were calculated by listing the co-occurrence of lithologies for each column of the model, assuming dredges sample the whole vertical extent of the model, and calculating a table as for the dredge data. The back-tilted sequence and the later normal fault create lithological associations which resemble the data to some extent, though clearly not fully. In model B the upper section is shifted sideways to simulate a potential effect of klippen of hanging wall rocks above detachment faults [*Cann et al.*, 1997; *Tucholke et al.*, 1998] and provides an improved match to the dredge table. These results do not, of course, show that the crust is as shown by these models but rather that multiple low-angle faulting or isolated klippen, combined with other effects (mass wasting, high-angle faulting, and intrusive complexities) are easily sufficient to explain the level of complexity in the dredge tables for transform valleys.

### 7.2. Effects of Slope Failures

Sedimentary breccias in five out of the six off-axis DSDP sites where gabbroic and ultramafic rocks were recovered (section 6) suggest that slope failures are important for transporting ultramafic and gabbroic rock debris into the active median valley floor, where they can be overlain by lavas. Sedimentary processes could therefore be important for creating anomalous associations between S, G, and E in dredge hauls, in addition to the accepted tectonic and magmatic processes discussed earlier. With abundant talus and sediment cover on the seafloor, slide blocks may be difficult to tell apart from in situ outcrop from within a submersible [*Karson*, 1998], so it is possible that sedimentary processes have also affected some dive observations.

It is well known that slope failures in the walls of transform valleys lead to abundant, commonly polymict sedimentary

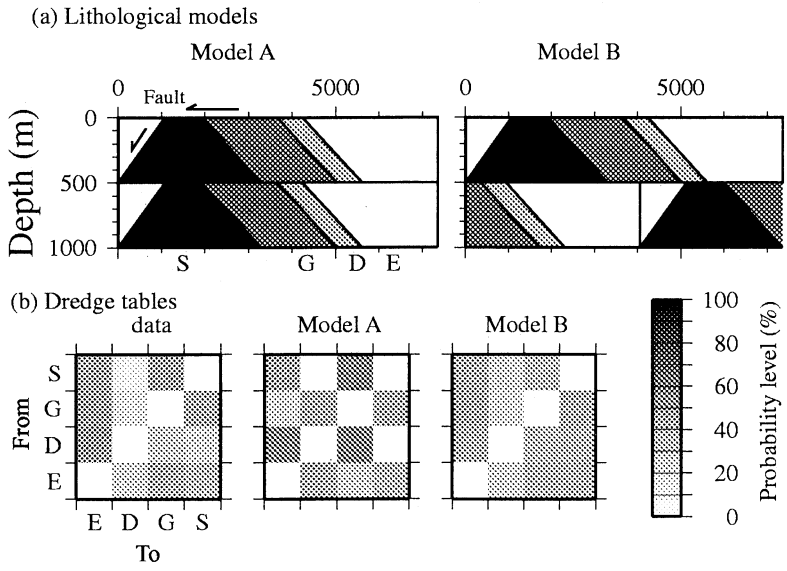


**Figure 11.** Detachment fault models and dredged tables. (a) Simplified lithological models for outcrop along a transform valley wall (5X vertical exaggeration) with lithologies in the proportions given by set 5 of Figure 5. Model A consists of units exposed by a low-angle detachment fault dipping to the left and tilting the lithologic units down to the right. The fault is subsequently offset by a perpendicular high-angle normal fault into the transform valley (striking parallel to the page) so that the high-level sequence is repeated in the valley wall below 500 m. Model B has a secondary low-angle detachment fault or klippen, causing the lithological section to repeat as in model A but with a lateral offset (serpentinite, solid; gabbro, dark shading; dikes, light shading; and open, extrusives). (b) Dredge cooccurrences (Figure 6e) compared to tables generated by assuming dredges sample all lithologies in any vertical section of the models. Although it is not suggested that the dredge and dive data actually reflect the structures shown in models A and B, the fact that model B is able to reproduce the tables shows that tectonic and magmatic processes are easily able to produce the level of complexity represented by the dredge tables.

breccias in transform valley floors [*Dick et al.*, 1991; *OTTER Team*, 1985; *Swift*, 1991]. *Tucholke* [1992], however, reported a 19 $km^3$ debris avalanche in a median valley wall scarp with a runout distance of at least 11 km. Recent deep-tow side-scan sonar images also show common slope failure deposits in the median valley, especially below large faults at segment ends, where serpentinites and gabbro are often sampled [e.g., *Allerton et al.*, 1995; *Blackman et al.*, 1998; *Escartin et al.*, 1999].

The sonar images and sampling may underrepresent the areas potentially covered by the debris because they could be overlain by axial valley lava. Assuming that subaerial volcanic debris avalanches are useful analogues of avalanches at mid-ocean ridges (subaerial and submarine volcanic avalanches have similar runout distances [*Lipman et al.*, 1988; W.B. Dade, pers. comm., 1999]), runout distances are expected to be 5-10 times their collapse heights [*Ui et al.*, 1986] for rock volumes of 0.1-1.0 $km^3$. Collapse of 100-1000 m high median valley escarpments would send material 1-10 km across the axial valley floor, potentially reaching the neovolcanic zone. Such material may become interbedded with lava flows in the subsiding hanging walls of the axial valley wall faults, as suggested by the stratigraphy in Figure 9. Thus sedimentary processes could be more generally important for incorporating serpentinite and gabbro into the shallow volcanic crust than originally thought and could potentially affect the heterogeneity observed at the surface, especially as recorded by dredging.

### 7.3. Characteristic Sequences on Slopes

A closer examination of the transition probability tables shows that while they support crustal models such as Figure 10b over Figure 10a, they do not reveal any common sequence of units on slopes. Figure 12 (left) shows the down slope tables compared to model tables (Figure 12, middle) derived by assuming a purely random arrangement of lithologies in which the model frequencies merely reflect the relative abundance of the different lithological units. The chance of encountering dikes after extrusives, for example, then reflects the number of dike units relative to gabbro and serpentinite units. (Abundances were calculated by inversely weighting each unit occurrence in Figure 3 and in the supplementary data by the number of dives in each 20 by 20 km area in order to be consistent with the data tables. Units were counted only if more than one unit occurred in a dive profile.) Figures 12a and 12b show some differences between the model and data tables, but combining data from both Figures 12a and 12b produces a table that is little different from a random model (Figure 12c), so the apparent differences in Figures 12a and 12b are probably artifacts of small sample size. The model and data tables in Figure 12c were tested using equation (2), omitting the factor of 2 in the denominator because the transition tables are not symmetrical. The weighted counts in the data tables were scaled so that the sum of each row equaled the total number of transitions for that row without weighting and placed in $C_{ij}$ of equation (2). Table elements were grouped to ensure that no elements had less than five counts, leaving eight grouped elements. The result suggests that the tables are just statistically different at $\chi_2^2$=18.0 (compared to the 5% critical value of 14.07 expected for 7 degrees of freedom), but the main cause of the difference is only 8 G→S transitions, of which three were from the well-sedimented Mid-Cayman Spreading Center [*Stroup and Fox*, 1981].

The frequencies in Figure 7 therefore mostly reflect the relative abundances of the different rock units rather than any

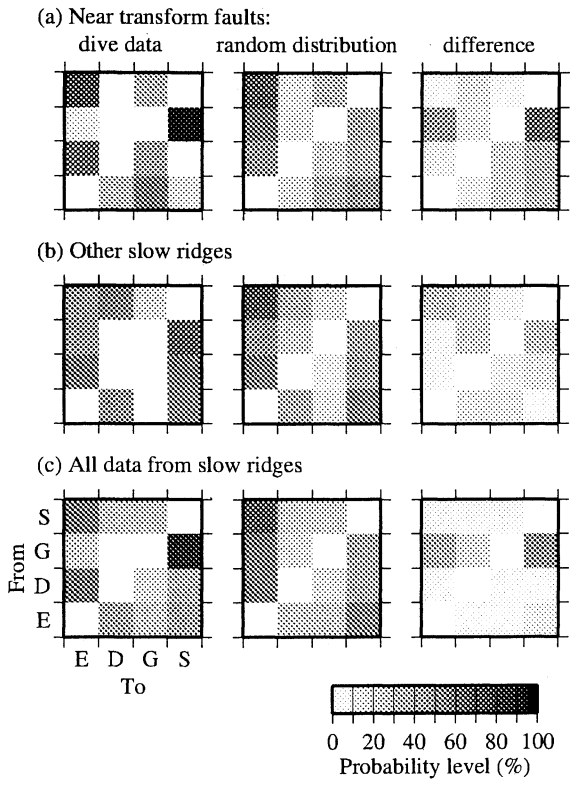


**Figure 12.** Transition probability tables for the Atlantic dive data compared to model tables calculated for a random distribution of lithologies. (left) (a) and (b) Weighted tables from Figures 6a and 6b and (c) derived by combining the two tables. (middle) Model tables calculated from the relative abundance of the different units (e.g., the probability of encountering S after E reflects the number of S units relative to D and G units). (right) Differences between the probabilities in the model and data tables. The transitions for Figure 12c, which has the largest sample size, are similar to those expected from a random arrangement of units and hence show that there is no currently detectable characteristic sequence of lithologies on Mid-Atlantic Ridge slopes.

preferred tendency for them to be associated. The lack of any anomalously common sequence could reflect the observational difficulties of the dive scientists involved in creating the original data and in converting the dive observations into discrete lithologic classes. However, if any underlying sequence were particularly common, some effect would be expected to be found in the tables. A further possible objection is that the method ignores the sizes of units. The database is inadequate to weight transitions by the widths of units (dives commonly terminate prematurely within units), but unit size is probably not important because the histograms of unit distances are similar for dikes, gabbro and serpentinite (Figure 4).

The resulting impression from Figure 7 and from the original dive profiles in Figure 2 therefore is that slow spreading oceanic crust is highly heterogeneous in terms of transition tables as well as in geological interpretations [*Karson*, 1998]. If there is an underlying preferred sequence of rock types exposed on slopes, it is uncommon and much less preferred to a random sequence. Since the analysis was based on immediate transitions between lithologies, this conclusion reflects the small-scale heterogeneity of rock types at the surface. However, if slow spreading oceanic crust is also heterogeneous at a larger scale, such as associated with temporal variations in melt supply to the ridge axis or sequential development of large-offset faults, the effect of large-scale heterogeneity also needs to be addressed. The competing crustal models in Figure 1 could be discriminated by determining whether slow-spread crust contains a laterally continuous sheeted dike layer; such a layer should exist in the model in Figure 1a but not in that shown in Figure 1b. Dive observations from a small number of ridge segments, however, may not favor one model over the other because they could merely reflect large-scale heterogeneity. Some effort to develop robust quantitative methods to characterize large-scale heterogeneity as well as small-scale heterogeneity will be required in order to address the general question of slow spreading crustal structure.

Geological cross sections created using a series of dives and extensive dredge hauls, with associated studies of rock fabrics and metamorphic history, can reveal much more about the geological history of an area and also allow inferences on crustal structure than the single dive profiles studied here. Accurate cross sections require sufficient observations from sonar and other methods to adequately characterize their geological environment, but such data are unfortunately very rare except in a few areas such as the Kane fracture zone [*Mevel et al.*, 1991; *Karson and Lawrence*, 1997b; *Auzende et al.*, 1989]. Rather than addressing the general issue of crustal structure, such efforts need to address small-scale problems that are tractable (e.g., the structure of an individual detachment fault), which over time should provide sufficient data eventually to address the more general question of slow spreading crustal structure.

## 8. Conclusions

Transition probability tables generated from dive observations show that extrusives to dikes, extrusives to gabbro, and extrusives to serpentinite are all common transitions down slopes of the Mid-Atlantic Ridge. These results are consistent with the view that ultramafic and gabbroic rocks can occur at shallow crustal levels, where they are commonly overlain by a thin carapace of basaltic extrusives and breccias. The tables are, however, also similar to tables generated assuming a purely random distribution of lithologies on slopes. Common transitions between extrusives and serpentinite, for example, reflect the high abundance of those two lithologies, rather than any preferred tendency for them to be associated.

The reason for the observed heterogeneity is partly the complex history of tectonic and magmatic events that create and affect slow spreading oceanic crust [e.g., *Karson*, 1998], but sedimentary processes may also contribute. In five out of the six off-axis drill sites where deep crustal and mantle rocks have been recovered, the deep lithologies occur as sedimentary breccias interbedded with lavas. Considering the abundant evidence for slope failures in side-scan sonar images, this suggests that failure of serpentinite or gabbro escarpments allows deep lithologies to be transported onto the median valley floor. There the debris is incorporated into the shallow volcanic crust and is responsible for some of the diversity of lithologies in rock dredges.

Dive observations are progressively revealing that slow spreading oceanic crust is highly complex, and it is therefore difficult to generalize crustal structure from the limited geological observations. However, in turning dive observations into a quantity that can be shown graphically and tested using statistics (here, transition probability tables), much of the information from the dives is lost (such as their local geological

contexts, types of contacts, and geological history revealed by petrology). Numerical methods will not provide satisfactory resolutions of the internal structure of slow spreading oceanic crust. This study will hopefully be useful, however, in highlighting the problems associated with the heterogeneity. The result here is based on immediate contacts between rock types, so it characterizes the finer scale heterogeneity of surface rock types. There may also be a larger scale heterogeneity as well, so locating the presence or absence of a sheeted dike complex (a key observation for discriminating the different models) could merely reflect differences between areas. It will thus be important to develop ways of characterizing large-scale heterogeneity if crustal structure is to be addressed adequately.

**Acknowledgments.** I thank Brian Tucholke for supplying a source listing of dredge data [*Tucholke and Lin*, 1994]. Laurence Coogan, Kathy Gillis, and an anonymous reviewer are thanked for reviewing this paper. A helpful review of an earlier version by Joe Cann is acknowledged. Many of the figures were prepared with the GMT software package [*Wessel and Smith*, 1991]. This work was supported by a Royal Society University Research Fellowship.

## References

Allerton, S., B.J. Murton, R.C. Searle, and M. Jones, Extensional faulting and segmentation of the Mid-Atlantic Ridge north of the Kane fracture zone (24° 00'N to 24° 40'N), *Mar. Geophys. Res.*, *17*, 37-61, 1995.

Aumento, F., and W.G. Melson, *Initial Reports of the Deep Sea Drilling Project*, vol. 37, U.S. Govt. Printing Office, Washington, D.C., 1977.

Auzende, J.-M., D. Bideau, E. Bonatti, M. Cannat, J. Honnorez, Y. Lagabrielle, J. Malavieille, V. Mamaloukas-Frangoulis, and C. Mevel, Direct observation of a section though slow-spreading oceanic crust, *Nature*, *337*, 726-729, 1989.

Auzende, J.-M., M. Cannat, P. Gente, J.-P. Henriet, T. Juteau, J. Karson, Y. Lagabrielle, C. Mevel, and M. Tivey, Observations of sections of oceanic crust and mantle cropping out on the southern wall of Kane FZ (N. Atlantic), *Terra Nova*, *6*, 143-148, 1994.

Barclay, A.H., D.R. Toomey, and S.C. Solomon, Seismic structure and crustal magmatism at the Mid-Atlantic Ridge, 35°N, *J. Geophys. Res.*, *103*, 17,827-17,844, 1998.

Blackman, D.K., J.R. Cann, B. Janssen, and D.K. Smith, Origin of extensional core complexes: Evidence from the Mid-Atlantic Ridge at Atlantis Fracture Zone, *J. Geophys. Res.*, *103*, 21,315-21,333, 1998.

Bloomer, S.H., P.S. Meyer, H.J.B. Dick, K. Ozawa, and J.H. Natland, Textural and mineralogical variations in gabbroic rocks from Hole 735B, *Proc. Ocean Drill. Program Sci. Results*, *118*, 21-39, 1991.

Bougault, H., and S.C. Cande, *Initial Reports of the Deep Sea Drilling Project*, 82, U.S. Govt. Print. Off., Washington, D.C., 1985.

Cande, S.C., R.C. Searle, and I. Hill, Tectonic fabric of the seafloor near north central Atlantic drill sites, *Initial Rep. Deep Sea Drill. Proj.*, 82, 17-33, 1985.

Cann, J.R., D.K. Smith, B. Brooks, M. Dougherty, S. Garland, J. Keeton, J. Lin, E. McAllister, C. MacLeod, R. Pascoe, and S. Spencer, Building the crust of the Mid-Atlantic Ridge, cruise report, Univ. of Leeds, England, 1992.

Cann, J.R., D.K. Blackman, D.K. Smith, E. McAllister, B. Janssen, S. Mello, E. Avgerinos, A.R. Pascoe, and J. Escartin, Corrugated slip surfaces formed at ridge-transform intersections on the Mid-Atlantic Ridge, *Nature*, *385*, 329-332, 1997.

Cannat, M., Emplacement of mantle rocks in the seafloor of the mid-ocean ridge, *J. Geophys. Res.*, *98*, 4163-4172, 1993.

Cannat, M., How thick is the magmatic crust at slow spreading oceanic ridges, *J. Geophys. Res.*, *101*, 2847-2857, 1996.

Cannat, M., et al., Thin crust, ultramafic exposures, and rugged faulting patterns at the Mid-Atlantic Ridge (22°-24°N), *Geology*, *23*, 49-52, 1995.

Cannat, M., Y. Lagabrielle, H. Bougault, J. Casey, N. de Coutures, L. Dmitriev, and Y. Fouquet, Ultramafic and gabbroic exposures at the Mid-Atlantic Ridge: Geological mapping in the 15°N region, *Tectonophysics*, *279*, 193-213, 1997.

Dick, H.J.B., Abyssal peridotites, very slow spreading ridges and ocean ridge magmatism, in *Magmatism in the Ocean Basins*, edited by A.D. Saunders and M.J. Norry, *Geol. Soc. Spec. Publ. 42*, 71-105, 1989.

Dick, H.J.B., W.B. Bryan, and G. Thompson, Low-angle faulting and steady-state emplacement of plutonic rocks at ridge-transform intersections, *Eos Trans. AGU*, *62*, 406, 1981.

Dick, H.J.B., H. Schouten, P.S. Meyer, D.G. Gallo, H. Bergh, R. Tyce, P. Patriat, K.T.M. Johnson, J. Snow, and A. Fisher, Tectonic evolution of the Atlantis II fracture zone, *Proc. Ocean Drill. Program Sci. Results*, *118*, 359-398, 1991.

Engel, C.G., and R.L. Fisher, Granitic to ultramafic rock complexes of the Indian Ocean ridge system, western Indian Ocean, *Geol. Soc. Am. Bull.*, *86*, 1553-1578, 1975.

Escartin, J., P.A. Cowie, R.C. Searle, S. Allerton, N.C. Mitchell, C.J. MacLeod, and A.P. Slootweg, Quantifying tectonic and magmatic strain at a slow spreading ridge segment (Mid-Atlantic Ridge, 29°N), *J. Geophys. Res.*, *104*, 10,421-10,437, 1999.

Fox, P.J., R.S. Detrick, and G.M. Purdy, Evidence for crustal thinning near fracture zones: Implications for ophiolites, in *Ophiolites; Proceedings International Ophiolite Symposium, Cyprus 1979*, edited by A. Panayiotou, pp. 161-168, Minist. of Agric. and Nat. Resour., Geol. Surv. Dep., Nicosia, Cyprus, 1980.

Francheteau, J., P. Choukroune, R. Hekinian, X. Le Pichon, and H.D. Needham, Oceanic fracture zones do not provide deep sections in the crust, *Can. J. Earth Sci.*, *13*, 1223-1235, 1976.

Gracia, E., D. Bideau, R. Hekinian, Y. Lagabrielle, and L.M. Parson, Along-axis magmatic oscillations and exposure of ultramafic rocks in a second-order segment of the Mid-Atlantic Ridge (33°43'N to 34°07'N), *Geology*, *25*, 1059-1062, 1997.

Hussong, D.M., P.B. Fryer, J.D. Tuthill, and L.K. Wipperman, The geological and geophysical setting near DSDP Site 395, North Atlantic Ocean, in *Initial Rep. Deep Sea Drill. Proj. 45*, 23-37, 1979.

Jaraslow, G.E., G. Hirth, and H.J.B. Dick, Abyssal peridotite mylonites: Implications for grain-size sensitive flow and strain localization in the oceanic lithosphere, *Tectonophyics*, *256*, 17-37, 1996.

Juteau, T., M. Cannat, and Y. Lagabrielle, Serpentinized peridotites in the upper oceanic crust away from transform zones: A comparison of the results of previous DSDP and ODP legs, *Proc. Ocean Drill. Program Sci. Results*, *106/109*, 303-308, 1990.

Karson, J.A., Seafloor spreading on the Mid-Atlantic Ridge: Implications for the structure of ophiolites and oceanic lithosphere produced in slow-spreading environments, in *Proceedings of the Symposium TROODOS 1987*, edited by J. Malpas, et al., pp. 547-555, Geol. Surv. Dep., Nicosia, Cyprus, 1990.

Karson, J.A., Internal structure of oceanic lithosphere: A perspective from tectonic windows, in *Faulting and Magmatism at Mid-Ocean Ridges, Geophys. Monogr. Ser.*, vol. 106, edited by W.R. Buck et al., pp. 177-218, AGU, Washington, D. C., 1998.

Karson, J.A., and H.J.B. Dick, Tectonics of ridge-transform intersections at the Kane fracture zone, *Mar. Geophys. Res.*, *6*, 51-98, 1983.

Karson, J.A., and R.M. Lawrence, Tectonic setting of serpentinite exposures on the western median valley wall of the MARK area in the vicinity of site 920, *Proc. Ocean Drill. Program, Sci. Res.*, *153*, 5-21, 1997a.

Karson, J.A., and R.M. Lawrence, Tectonic window into gabbroic rocks of the middle oceanic crust in the MARK area near Sites 921-924, *Proc. Ocean Drill. Program Sci. Res.*, *153*, 61-76, 1997b.

Kong, L.S.L., S.C. Solomon, and G.M. Purdy, Microearthquake characteristics of a mid-ocean ridge along-axis high, *J. Geophys. Res.*, *97*, 1659-1685, 1992.

Lagabrielle, Y., and M. Cannat, Alpine Jurassic ophiolites resemble the modern central Atlantic basement, *Geology*, *18*, 319-322, 1990.

Lagabrielle, Y., D. Bideau, M. Cannat, J.A. Karson, and C. Mevel, Ultramafic-mafic plutonic rock suites exposed along the Mid-Atlantic Ridge (10°N-30°N). Symmetrical-asymmetrical distribution and implications for seafloor spreading processes, in *Faulting and Magmatism at Mid-Ocean Ridges, Geophys. Monogr. Ser.*, vol. 106, edited by W.R. Buck et al., pp. 153-176, AGU, Washington, D. C., 1998.

Lipman, P.W., W.R. Normark, J.G. Moore, J.B. Wilson, and C.E. Gutmacher, The giant submarine Alika debris slide, Mauna Loa, Hawaii, *J. Geophys. Res.*, *93*, 4279-4299, 1988.

Melson, W.G., and P.D. Rabinowitz, Initial Reports of the Deep Sea Drilling Project, vol. 45, U.S. Govt. Print. Off., Washington, D.C., 1979.

Mevel, C., M. Cannat, P. Gente, E. Marion, J.M. Auzende, and J.A.

Karson, Emplacement of deep crustal and mantle rocks on the west median valley of the MARK area (MAR, 23°N), *Tectonophysics*, *190*, 31-53, 1991.

Miller, I., and J.E. Freund, *Probability and Statistics for Engineers*, Prentice-Hall, Old Tappan, N. J., 1965.

Mitchell, N.C., J. Escartin, and S. Allerton, Detachment faults at mid-ocean ridges garner interest, *Eos, Trans. AGU*, *79(10)*, 127, 1998.

Mitchell, N.C., M.A. Tivey, and P. Gente, Slopes of mid-ocean ridge fault scarps from submersible observations, *Earth Planet. Sci. Lett.*, *183*, 543-555, 2000.

Muller, R.D., W.R. Roest, J.-Y. Roger, L.M. Gahagan, and J.G. Sclater, Digital isochrons of the world's ocean floor, *J. Geophys. Res.*, *102*, 3211-3214, 1997.

Nisbet, E.G., and C.M.R. Fowler, The Mid-Atlantic Ridge at 37 and 45°N: Some geophysical and petrological constraints, *Geophys. J. R. Astron. Soc.*, *54*, 631-660, 1978.

OTTER Team, The geology of the Oceanographer Transform: The transform domain, *Mar. Geophys. Res.*, *7*, 329-358, 1985.

Pederson, R.B., The nature and significance of magma chamber margins in ophiolites: Examples from the Norwegian Caledonides, *Earth Planet. Sci. Lett.*, *77*, 100-112, 1986.

Penrose Conference Participants, Ophiolites, *Geotimes*, *17*, 24-25, 1972.

Potter, P.W., and R.F. Blakely, Random processes and lithologic transitions, *J. Geol.*, *76*, 154-170, 1968.

Sandwell, D.T., and W.H.F. Smith, Marine gravity anomaly from Geosat and ERS-1 satellite altimetry, *J. Geophys. Res.*, *102*, 10,039-10,054, 1997.

Schulz, N.J., R.S. Detrick, and S.P. Miller, Two- and three-dimensional inversions of magnetic anomalies in the MARK area (Mid-Atlantic Ridge 23°N), *Mar. Geophys. Res.*, *10*, 41-57, 1988.

Selley, R.C., Studies of sequences in sediments using a simple mathematical device, *Q. J. Geol. Soc. London*, *125*, 557-581, 1969.

Sleep, N.H., and G.A. Barth, The nature of oceanic lower crust and shallow mantle emplaced at low spreading rates, *Tectonophysics*, *279*, 181-191, 1997.

Stroup, J.B., and P.J. Fox, Geologic investigations in the Cayman Trough: Evidence for thin oceanic crust along the Mid-Cayman Rise, *J. Geol.*, *89*, 395-420, 1981.

Swift, S.A., Gravels in the Atlantis II fracture zone, *Proc. Ocean Drill. Program Sci. Results*, *118*, 431-438, 1991.

Tucholke, B.E., Massive submarine rockslide in the rift-valley wall of the Mid-Atlantic Ridge, *Geology*, *20*, 129-132, 1992.

Tucholke, B.E., and J. Lin, A geological model for the structure of ridge segments in slow spreading ocean crust, *J. Geophys. Res.*, *99*, 11,937-11,958, 1994.

Tucholke, B.E., J. Lin, and M.C. Kleinrock, Mullions, megamullions, and metamorphic cores complexes on the Mid-Atlantic Ridge, *Eos Trans. AGU*, *77(46)*, Fall Meet. Suppl., F724, 1996.

Tucholke, B.E., J. Lin, and M.C. Kleinrock, Megamullions and mullion structure defining oceanic metamorphic core complexes on the Mid-Atlantic Ridge, *J. Geophys. Res.*, *103*, 9857-9866, 1998.

Ui, T., H. Yamato, and K. Suzuki-Kamata, Characterization of debris avalanche deposits in Japan, *J. Volcanol. Geotherm. Res.*, *29*, 231-243, 1986.

Wessel, P., and W.H.F. Smith, Free software helps map and display data, *Eos Trans. AGU*, *72*, 441, 445-446, 1991.

---

N. C. Mitchell, Department of Earth Sciences, Cardiff University, P.O. Box 914, Cardiff CF10 3YE, Wales, UK. (neil@ocean.cardiff.ac.uk)

(Received September 11, 2000; revised June 8, 2001;
accepted June 9, 2001.)